Target rotation parameter estimation for ISAR imaging via frame processing

Xuezhi Wang[1], Yajing Huang[2], Weiping Yang[2], Bill Moran[1]

(1. School of Electrical and Computer Engineering, RMIT University, Australia; 2. School of Electronic Science and Engineering, National University of Defense Technology, Changsha 410073, China)

Abstract: Frame processing method offers a model-based approach to Inverse Synthetic Aperture Radar (ISAR) imaging. It also provides a way to estimate the rotation rate of a non-cooperative target from radar returns via the frame operator properties. In this paper, the relationship between the best achievable ISAR image and the reconstructed image from radar returns was derived in the framework of Finite Frame Processing theory. We show that image defocusing caused by the use of an incorrect target rotation rate is interpreted under the FP method as a frame operator mismatch problem which causes energy dispersion. The unknown target rotation rate may be computed by optimizing the frame operator via a prominent point. Consequently, a prominent intensity maximization method in FP framework was proposed to estimate the underlying target rotation rate from radar returns. In addition, an image filtering technique was implemented to assist searching for a prominent point in practice. The proposed method is justified via a simulation analysis on the performance of FP imaging versus target rotation rate error. Effectiveness of the proposed method is also confirmed from real ISAR data experiments.

Key words: ISAR imaging;　frame theory;　frame processing;　target rotation rate;　radar waveforms

CLC number: TN95　　**Document code:** A　　**DOI**：10.3788/IRLA201645.0302001

0 Introduction

The rotational motion of a target in ISAR imaging is typically described using the target rotation rate, which is approximately constant during a very short signal accumulation period. For non-cooperative targets, estimating the underlying target rotational motion from radar returns is in general difficult. While ISAR imaging using an incorrect target rotation rate will cause image distortion, the distortion behavior varies depending on the processing method used. A number of researchers have addressed the problem using techniques from sensor array processing [1-4], where the time-space structure of the radar signal is explored via multiple known prominent image points [1]. The rotation rate of a target may be computed by exploring the phase slope difference between two prominent points from an ISAR snapshot of the target[5], or from the geometric constraints between prominent points in a sequence of ISAR snapshots[6]. While various approaches with a certain degree of success are found in the literature, fundamental research on this issue still remains challenging. In particular, a clear understanding of the relation between the quality of the reconstructed image, target rotation rate, and radar returns is needed. Following our earlier work in[7-8], in this paper, we address the target rotation rate estimation problem using the frame processing framework.

A direct 2D FFT is the most popular technique for ISAR imaging. This interprets the complex signal sequence of radar returns in a uniform grid far-field Range-Doppler plane [9]. ISAR imaging can also be performed using the so called back projection (BP) or convolution back projection (CBP) methods [10-11]. The latter are based on the computer-aided-tomography (CAT) idea and implemented by fast Radon transform. While the Radon transform based approaches can avoid range walk problem with a large antenna aperture, it has a closed relation with FFT based techniques. The frame processing (FP) method proposed in[7,12] is a model-based ISAR imaging technique derived using Frame theory and is an effective alternative to FFT−based methods where the range walk problem associated with FFT based methods is no longer an issue. The fundamental difference between the FP and FFT methods is the way that the cross-range information of a target is recovered from the radar returns [2]. The former is based on a target rotation model embedded in the returns while the latter is based on the Doppler shift between radar pulses.

Frame theory, which is abstracted from the fundamental notion in Gabor′s work on signal processing in Ref.[13], was introduced by Duffin and Schaeffer in 1952 in Ref.[14]. It is a fundamental mathematical tool for decomposing signals into finite dimension elemental signals. In our context, these elemental signals are related to the pixels of reconstructed image in radar imaging. The FP approach considers radar returns as vectors in a Hilbert space where the frame, which spans the space, is specified. The ISAR imaging is done via the projection of radar returns onto the frame viewed in the range-Doppler plane. The FP method solves the issue of range walk, sometimes called "migration through a resolution cell", which is a problem present in FFT based imaging methods. The FP method is capable of reconstructing a target imaging in more detail by using a longer radar return sequence.

Fundamentally, the FP imaging procedure can be seen as a model-based estimation process which produces an image of a target from radar returns

1 A prominent image point in the context of this paper means an image point at which the intensity amplitude is significantly higher than those of its neighbors.

2 In this paper, the radar returns are specifically the sequence of radar returns after compensated via a target motion compensation (TMC) program and contain only target rotational motion.

based on a target rotation model. A rotation rate dependent signal structure is embedded in the frame constructed in radar data space and knowledge of target rotation rate is thus explicitly required for building a dual frame, which is the key tool reconstructing the target image from the returns. Fig.1 highlights the major differences between the FP method and FFT based technique using a flowchart of the two imaging processing methods. Radar returns for ISAR imaging are assumed to have been pre-processed so that they only contain the dechirping output signals resulting from target rotational motion. It is well understood that the signal components corresponding to target rotational motion can be extracted from total target returns via the technique of translational motion compensation (TMC) which has been extensively studied in Ref. [15−16]. We will make this assumption throughout the entire paper. As shown in the left column of Fig.1, the pre-processing consists of demodulation, dechirping and target tracking and motion analysis three major components. As with other ISAR imaging techniques, in this work we also assume that (1) the underlying ISAR imaging system satisfies the far field condition ($r_0 \gg \Delta r$); (2) target rotation rate within the signal period remains constant; (3) the target Doppler shift within a single radar pulse remains constant.
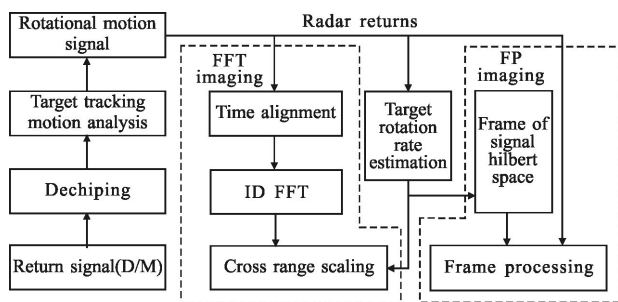

Fig.1 ISAR imaging: FFT−based methods vs the frame processing (FP) method. The pre-processing of received signals is indicated by the left column. Radar returns in this paper means the output of target rotational motion signal component

In this paper, the problem of estimating target rotation rate from radar returns for ISAR imaging using the FP method is explored. We derive and analyze a pixelwise relationship between radar returns of a target and its ISAR image in terms of the frame operator of a Hilbert space (Section II). This relationship provides an interesting view of image focus with respect to target rotation rate under FP ISAR imaging. Based on the analysis, a practical procedure under the FP method for target rotation rate estimation based on a prominent image point is presented. The algorithm is justified using the result of Monte Carlo simulation for the estimation of target rotation rate in a random scenario (Section III). The major contributions of this paper are

(1) derivation of a relationship between the reconstructed and the best achievable target images in terms of the frame operator. In the FP method, radar returns are mapped onto the image space spanned by the underlying frame via frame operators;

(2) demonstration that image defocusing under the FP method can be interpreted as a consequence of frame operator mismatch, which yields a potential to use the frame structure of radar returns for the estimation of rotation vector magnitude of a target under the FP method;

(3) proposal of a procedure for estimating target rotation rate from radar returns at a prominent image point and a practical method for identifying a prominent point;

(4) justification of the proposed target rotation vector magnitude method via Monte Carlo multiple runs under a random ISAR imaging scenario, as well as with real data.

We point out that considerable research efforts have also been devoted on improving the efficiency of radar imaging. Various sparse imaging techniques address the optimization of computational issues statistically for a given vector based algorithm using the idea of compressive sensing[17], random projection or orthogonal matching pursuit[18]. While frames are prominent in the theory compressive sensing, their use in FP is quite different from their use in that theory.

Here we make no sparsity assumptions. As our primary interest is in the fundamental imaging concept and the subsequent rotation rate estimation technique in the FP method and thus will not cover this topic in this work.

1　ISAR imaging via frame processing

A frame is defined[14] as a set of elements $\{i_k\}$ of the vector $I \in H$ in a complex Hilbert space H which satisfies the following frame condition:

The system $\{i_k\}$ is a frame of H if there exist $0 < A \leqslant B < \infty$ (lower and upper bounds) such that

$$A\|I\|^2 \leqslant \sum_k |\langle I, i_k \rangle|^2 \leqslant B\|I\|^2, \ \forall I \in H \tag{1}$$

An important property of frames is that the frame $\{i_k\}$ spans H. Consequently, a frame has the same properties as a basis in terms of reconstructing a vector from scalar products.

The ISAR imaging problem can be formulated and solved using frame theory. Let $J_N(\tau, \omega_0) \in H$ denote a sequence of N consecutive radar pulses reflected off a rotating target at rotation rate ω_0 where $\tau \in [0, T]$ is the radar fast time (round trip time) in a single pulse repeat period (PRT) denoted by T. We assume (see Fig.1), the radar returns $J_N(\tau, \omega_0)$ are the dechirping output and only contain the signal components related to target rotational motion. ISAR imaging means the reconstruction a tomographic image $S \in R^2$ of the target in a Range-Cross range plane by processing the radar returns $J_N(\tau, \omega_0)$. In the FP framework in Ref.[7], it is demonstrated that the ISAR image (vector) S of a target can be obtained by projecting radar returns $J_N(\tau, \omega_0)$ onto the frame I which spans the radar data (Hilbert) space H. Here an underline indicates a vector.

Without loss of generality, we assume that the signal return from a target occupies M signal range bins. The target image S on the spatial plane is of $M \times N$ pixels. The radar returns $J_N(\tau, \omega_0)$ and target image $S(\tau, \omega_0)$ are related by the following inner product[7]:

$$J_N(\tau, \omega_0) = \langle S(\tau, \omega_0), I(\tau, \omega_0) \rangle = \sum_{m=1}^{M} \sum_{n=1}^{N} S_{m,n}(\tau, \omega_0) I_{m,n}(\tau, \omega_0) \tag{2}$$

where the set of vectors

$$I = \{I_{m,n}(\tau, \omega_0)\}_{m \in M, n \in N} \in H \tag{3}$$

is the frame of the radar data space H. We emphasize that the frame $I(\tau, \omega_0)$ is determined by radar parameters and the underlying target rotation rate ω_0 [7]. An ISAR data frame example is given as follows. For a high resolution radar (HRR) with a Step Frequency (SF) waveform $w(t)$, i.e.,

$$w(t) = \sum_{k=0}^{N_f-1} e^{2\pi i(f_o + k\Delta f)t} \text{rect}\left(\frac{t - T_f/2 - kT_f}{T_f}\right) \tag{4}$$

where f_0 is the start frequency, Δf is the frequency step, T_f is the dwell time and the signal period is $T = N_f \cdot T_f$. The kth element of the frame of radar data space is given by

$$I_{m,n}^k(\tau, \omega) = B\text{sinc}(B(\tau - d_k^{m,n})) e^{2\pi i f_c(\tau + d_k^{m,n})}, \ k = 1, \cdots, N \tag{5}$$

where B is the bandwidth of the waveform, and

$$d_k^{m,n} \triangleq \frac{2r_{m,n}(t_k)}{c}, \ t_k \in [(k-1)t, kT] \tag{6}$$

is the time delay of the return signal from the (m,n)th scatterer[7]. $r_{m,n}(t_k)$ is a standard target rotation function given by

$$r_{m,n}(t_k) = r_0 + m\Delta x \cos\omega_0 t_k - n\Delta y \sin\omega_0 t_k \tag{7}$$

where r_0 is the range between radar and the center of target, $(\Delta x, \Delta y)$ represents the area of the scatterer at (m,n).

For non-cooperative targets, the rotation rate ω_0 is unknown and need to be estimated from the radar returns $J_N(\tau, \omega_0)$. We use ω to signify the case that the underlying target rotation rate ω_0 is an unknown parameter. Once the frame has been obtained in radar data space, the target image can be reconstructed from radar returns via the following frame decomposition

$$S(\tau, \omega_0) = F^{-1} F J_N(\tau, \omega_0) = \sum_{m=1}^{M} \sum_{n=1}^{N} \langle J_N(\tau, \omega_0), \tilde{I}_{m,n}(\tau, \omega_0) \rangle I_{m,n}(\tau, \omega_0) \tag{8}$$

$$\approx \sum_{m=1}^{M} \sum_{n=1}^{N} \langle J_N(\tau, \omega_0), \tilde{I}_{m,n}(\tau, \omega) \rangle I_{m,n}(\tau, \omega) \tag{9}$$

where the set $\tilde{I} = \{\tilde{I}_{m,n}(\tau, \omega)\}_{m \in M, n \in N}$ is the dual frame of $I(\tau, \omega)$[14]. In Eq.(8), S signifies that the image can be literally represented by a vector of dimension $M \times N$ in the Hilbert space spanned by the frame $I(\tau, \omega)$.

The inner product terms are called frame coefficients, and represent complex intensities of the constructed image. The dual frame element $\tilde{I}_{m,n}(\tau,\omega)$ is related to the frame element $I_{m,n}(\tau,\omega)$ by a frame operator, denoted by F, of the following form

$$\tilde{I}_{m,n}(\tau,\omega)=F^{-1}I_{m,n}(\tau,\omega) \tag{10}$$

The frame operator F is a positive, self-adjoint and invertible square matrix, defined by

$$F \triangleq I(\tau,\omega)I^H(\tau,\omega)=[I_1,\cdots,I_{MN}]^H[I_1,\cdots,I_{MN}] \tag{11}$$

where $[\cdot]^H$ signifies the conjugate transpose operation. From the definition (11), the (k,l)th entry of F is given by

$$F_{k,l}=\langle I_k(\tau,\omega),\tilde{I}_l(\tau,\omega)\rangle \tag{12}$$

Remarks:

The approximation from Eq.(8) to Eq.(9) reflects a practical procedure where the estimated rotation rate ω replaces ω_0 to build the dual frame $\tilde{I}_{m,n}(\tau,\omega)$. As we indicate later, the estimation error $|\omega_0-\omega|$ causes the constructed image defocusing.

The frame coefficients $\langle J_N(\tau,\omega),\tilde{I}_{m,n}(\tau,\omega)\rangle$ in Eq.(9) depend on the estimation error $|\omega_0-\omega|$ of the target rotation rate ω_0. As shown in the next section, we can utilize such signal structure to estimate the target rotation rate ω.

2 Rotation rate estimation in frame processing

As mentioned earlier, ISAR imaging under the FP approach can be thought as the projection of radar returns onto a locally rotating coordinate system, where the frame of radar returns serves as the base of such a system. It distinguishes itself from the Radon transform based approaches (e.g. BP/CBP) in that it embeds a rotating image pixelated grid system into the signal model of target radar returns as a frame, while Radon transform based techniques reconstruct the target image by the integration of individual slices observed by radar receiver. Radon transform techniques typically use the Fourier slice technique, which at least implicitly relies on a Fourier basis. In this section, the relationship between the intensities of the best achievable image and actual constructed image by the FP approach is derived. Based on this relationship, the quality of a reconstructed image versus the estimation error of target rotation rate is analyzed using simulated examples and some observations are discussed. Furthermore, a practical procedure for estimating target rotation rate from radar returns using the FP technique is presented and is statistically justified via a random ISAR imaging scenario.

In view of Eq.(9), the image amplitude at the (m,n)th pixel entry $(m \in M, n \in N)$ in the FP approach is given by

$$S_{m,n}=\langle J_N(\tau,\omega),\tilde{I}_{m,n}(\tau,\omega)\rangle \tag{13}$$

Substituting Eq.(2) into Eq.(13), we obtain

$$S_{m,n}(\tau,\omega)=\langle J_N(\tau,\omega_0),\tilde{I}_{m,n}(\tau,\omega)\rangle=$$

$$\langle \sum_{i=1}^{M}\sum_{j=1}^{N}S_{i,j}(\tau,\omega_0)I_{i,j}(\tau,\omega_0),\tilde{I}_{m,n}(\tau,\omega)\rangle= \tag{14}$$

$$\sum_{i=1}^{M}\sum_{j=1}^{N}S_{i,j}(\tau,\omega_0)\langle I_{i,j}(\tau,\omega_0),\tilde{I}_{m,n}(\tau,\omega)\rangle \tag{15}$$

Eq.(15) is a representation of ISAR image intensity at the (m,n)th pixel in terms of the frame of radar data space parameterized by the rotation rate of the underlying target. Reindexation into vector form $\{k=1,\cdots,MN\}$ from matrix form $\{m=1,\cdots,N; n=1,\cdots,N\}$ transforms Eq.(15) into

$$S_{m,n}(\tau,\omega) \equiv S_p(\tau,\omega)=\sum_{k=1}^{MN}S_k(\tau,\omega_0)F_{k,p}(\omega_0,\omega) \tag{16}$$

where $F_{k,p}(\omega_0,\omega)$ is defined by Eq.(12) as

$$F_{k,p}(\omega_0,\omega) \triangleq \langle I_k(\tau,\omega_0),\tilde{I}_p(\tau,\omega)\rangle \tag{17}$$

Eq.(16) shows the relationship between the frame coefficients of the radar returns and the frame operator. From this relationship, we make the following observations.

(1) Under the frame processing framework, the distortion of a reconstructed ISAR image is a consequence of the frame operator mismatch with respect to target rotation rate ω.

(2) The reconstructed image will be the best achievable image, i.e., $S_p(\tau,\omega)=S_p(\tau,\omega_0)$, if $\omega=\omega_0$, $w(t)=\delta(t)$ and $N\to\infty$. In this case, the frame operator F is an identity matrix. This also explains the finite resolution limitation of ISAR imaging technology, that is, for a fixed ω_0 and radar pulse repeat frequency the resolution of reconstructed ISAR image is limited by radar waveforms and the number of pulses considered.

(3) For HRR waveforms, their resulting pulse width is considerably narrow with respect to PRT. Therefore, F may be practically approximated by a diagonal matrix when $\omega_0=\omega$ for a large N.

(4) Image defocusing under FP reconstruction implies signal energy dispersal which is evidenced by the nonzero values of off-diagonal elements in F.

Next, we present two examples to demonstrate how the mismatch of target rotation rate would affect the properties of the frame operator, and thus the imaging quality. Based on the observations above, we outline an effective algorithm which estimates target rotation rate by maximising image intensity at a prominent point. By simulation, a statistical condition for estimating ω based on the maximization of the intensity of a prominent image point is discussed, which more or less justifies the signal based approaches for target rotation rate estimation in practical situation.

Figure 2 is a mesh plot of a frame operator for a 16×16 image vector space for radar returns generated based on a linear frequency modulated (LFM) waveform, where pixel scale is assumed to be one unit square. On this figure, we make the following remarks.

The frame operator will be a diagonal-dominated matrix (Fig.2(a)) only when the target rotation rate ω in the dual frame is identical to that in radar returns. In other words, the dual frame with a mismatched rotation rate results in a non-diagonal matrix for the associated frame operator.

The properties of a frame operator for ISAR data space can be potentially used for the estimation of

target rotation vector magnitude. As indicated in Eq.(15), a matched target rotation vector magnitude is used to construct the dual frame is a necessary condition for the reconstructed image intensity at a prominent point to be maximized as far as target rotation rate is concerned.
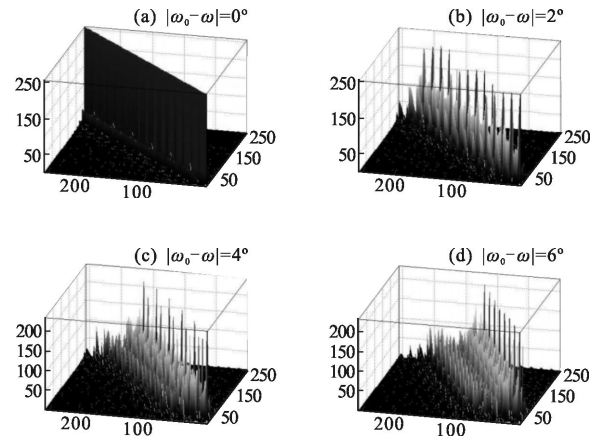

Fig.2 Values of the frame operator $F(\omega_0,\omega)$ for a 16×16 image vector space. The maximum height is 256 which is the dimension of the image vector

Figure 3 illustrates how the quality of an ISAR image changes when a mismatched target rotation rate is used to build the dual frame of radar data under FP imaging. The images are reconstructed based on a 16×16 frame operator from the original image using Eq.(16). We should emphasize that a mismatched target
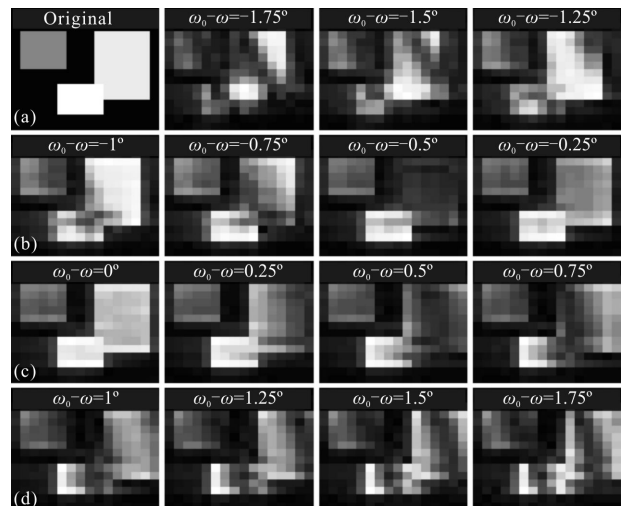

Fig.3 Image reconstruction using the FP method as in Eq.(16) vs the values of object rotation rate difference $\omega_0-\omega$ between ground truth ω_0 and the actual value ω used in the reconstruction, where radar data consists of total 256 pulses

rotation vector magnitude will alter the image intensity distribution because of signal energy dispersion, however, the scale of the target image will remain the same under the FP method. This is a major distinction between the FP method and FFT−based ISAR imaging methods.

From the above analysis we may conclude that ISAR imaging under FP can be regarded as a structured estimation problem where the rotation vector magnitude of the target is embedded in the structure of image reconstruction. A mismatch of target rotation rate in the dual frame built from radar returns for image reconstruction will change the image intensity distribution but not the scale of the target image. In particular, at a prominent image point the intensity achieves its maximum with a matched target rotation vector magnitude. Consequently, a practical procedure to estimate target rotation rate ω from radar returns using FP method can be outlined as follows.

Step 1: Obtain a snapshot of target image using FP (with a guessed target rotation rate ω).

Step 2: Identify a prominent image point (m,n). A prominent image point in this paper is defined as a point at which the intensity level is much higher than the intensities of its neighbors.

Step 3: At the prominent point (m,n), estimate ω by solve the following maximization problem

$$\omega=\underset{\omega^*}{\arg\max}\ \{S_{m,n}(\omega_0,\omega^*)\}=\omega_0 \tag{18}$$

which is equivalent to

$$\omega=\underset{\omega\in\Phi}{\arg\max}\ \|\langle J_N(\tau,\omega_0),\tilde{I}_{m,n}(\tau,\omega)\rangle\| \tag{19}$$

where Φ is a specified search range of ω, and $J_N(\tau,\omega_0)$ represents radar returns. $\tilde{I}_{m,n}(\tau,\omega)$ is the (m,n)th element of the dual frame which spans the underlying radar data space and it can be practically constructed based on radar parameters and knowledge of target rotation vector magnitude[7].

In practice, if a global maximum with respect to the rotation rate of target at an image point can be observed, the underlying image point is a prominent

3 The top view of those plots as shown in Fig.2.

point. A heuristic method for finding a prominent point is described in the next section.

The above proposed procedure is justified using the following random ISAR imaging example via Monte Carlo simulation statistics. In this example, the target image consists of 16×16 pixels with intensity values uniformly distributed, i.e., $S_{m,n}\in[0,1]$, $m,n=1,\cdots,16$. The ground truth target rotation rate is $\omega_0=10(°)/s$. At each run, a prominent image point (m_0,n_0) is generated with intensity value $S_{m0,n0}=0.96$, while the intensities of its neighborhood which consists of $(5\times5)-1$ pixels are all 0.3. Figure 4(a) shows the random image recorded from a particular run, where the prominent point is indicated by a yellow "+" and the color at each pixel signifies intensity value. Figure 4(b) shows the top view image[3] of the corresponding frame operator $(256\times256$ matrix), where those entries marked by short dashed lines correspond to the neighboring pixels centered at the pixel of the diagonal entry.
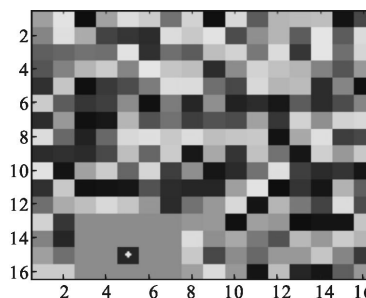
(a) Image of random noise with a prominent point
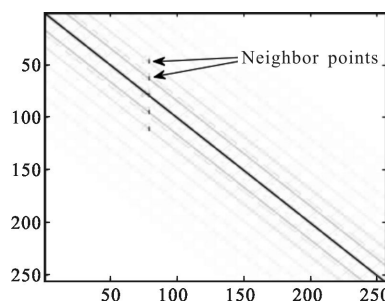
(b) Image of the frame operator when target rotation rate is matched

Fig.4 Illustration of a realization of the random ISAR imaging scenario involving a prominent image point

As we analyzed previously, the frame operator

with a mismatched ω will result in non-zero off-diagonal elements which means the intensity of the center pixel is influenced by the energies from its neighboring pixels. This "side-lobe effect" is a typical defocusing pattern under the FP imaging approach. Clearly, at a prominent point, lower side lobes are expected to eliminate the chance that the intensity maximization ends at a local maxima with respect to ω. In view of Eq.(16), the resulting image intensity at a specific point will depend largely on the diagonal element values in the frame operator corresponding to that point and the maximum value is achieved when the frame operator is matched, i.e., $\omega = \omega_0$. In consequence, the rotation rate of a target in ISAR imaging can be estimated by maximizing the intensity of a prominent point in the frame processing formulation.
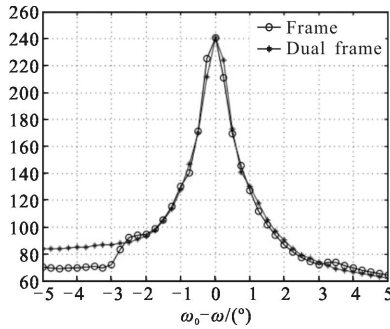
Figure 5 shows the histogram of target rotation

Fig.5 Histogram of the error distribution in the estimation of ω by maximizing the intensity of a prominent point over 1 000 runs in the random ISAR imaging scenario

rate estimation error over 1 000 runs and it represents the number of counts versus the error of the estimated target rotation vector magnitude. Clearly, the majority of runs yield small estimation errors by either frame or dual frame ω matching. This confirms the effectiveness of the proposed procedure for target rotation vector magnitude estimation via a prominent point. Under this scenario, the simulation result shows that more than 820 out of 1 000 runs are error free. Furthermore, if a non-zero error offset of $|\omega_0 - \omega| \leqslant 1°$ is allowed, the success rate of estimation will reach 98%. In practice, a prominent point on a snapshot

may be found via the method as described below.

3 Experimental results

In this section, we demonstrate further the proposed technique and procedure to estimate target rotation vector magnitude under FP ISAR imaging by using real data. Clearly, identification of a prominent scatterer on the target from radar returns is a necessary condition to enable this technique. Many image processing techniques, though not optimal, can be adopted to find a prominent point on a snapshot image. Here, we firstly describe a simple prominent point detection method which was considered in our subsequent experiment for the estimation of rotation vector magnitude of a Boeing 737 via radar returns using the proposed frame match idea.

A snapshot is a target ISAR image generated from its radar returns by using a guessed rotation vector magnitude. Let the (m,n)th intensity value of the snapshot S be written as $S_{m,n}$ and $A_{m,n}^{h}$ denote the mean intensity value over the neighboring rectangle area of the (m,n)th pixel, where the coordinates of the rectangle area are given by $H=:[m-h,m+h,n-h,n+h]$. The idea is to compute a map P of size S. Each pixel value $P_{m,n}$ on the map is the ratio of the intensity and average intensity over the neighboring area at the pixel on the snapshot, that is,

$$P_{m,n} = \frac{a_{m,n}}{A_{m,n}^{h}} \tag{20}$$

where

$$A_{m,n}^{h} = \frac{1}{|H|} \sum_{i,j \in H} a_{i,j} \tag{21}$$

$|H|$ signifies the number of pixels in H. All local prominent points can be identified on the map for a given threshold. In our experiment, the threshold is set to be $0.9 P_{max}$, where P_{max} is the maximum value of P and $h=10$.

Next, we present an experiment for estimating rotation vector magnitude using the proposed frame processing idea by analyzing real data for a Boeing

737 aircraft. This data has been provided by the Imaging Processing Laboratory in National University of Defence Technology. We take a sequence of $N=200$ radar returns (bursts) and extract the signals centered at the target in $M=200$ range bins. The radar uses a Step Frequency waveform of bandwidth $B=500$ MHz with center carrier frequency $f_0=9$ GHz and periodic repeat frequency $PRF=40$ kHz. Target rotation vector magnitude ω is unknown.

Figure 6(a) shows a snapshot of the ISAR image generated using the FP method by assuming $\omega=7(°)/s$. As shown in this figure, the green dot indicates the prominent point identified using the prominent search technique. Under the threshold of 90% of the maximum value of the computed map, the prominent point is found at the location(102,109) shown in Fig.6(b).
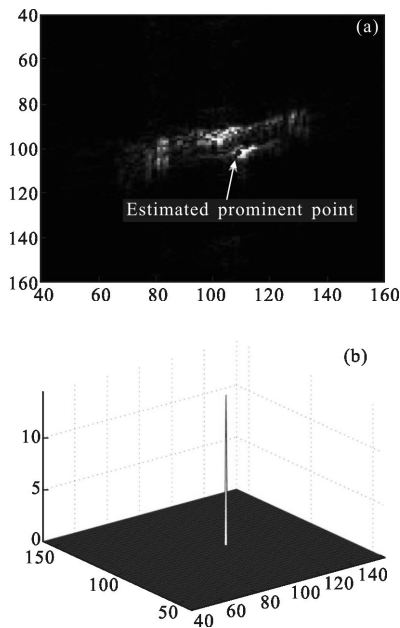

Fig.6 Estimated prominent point on the snapshot with a guessed target rotation rate $\omega=7(°)/s$ and demonstration of the prominent point estimation method

Figure 7 (a) illustrates that the intensity at the prominent point achieves a maximum when the target rotation rate ω is less than 2 (°)/s. In fact, when ω is in the region [0.5 (°)/s~2.4 (°)/s] and the ISAR images at this rotation vector magnitude range are almost the same as that at $\omega=1.1$ (°)/s (see Fig.8 (b)). The ISAR image produced by the standard 2D FFT with the same cross-

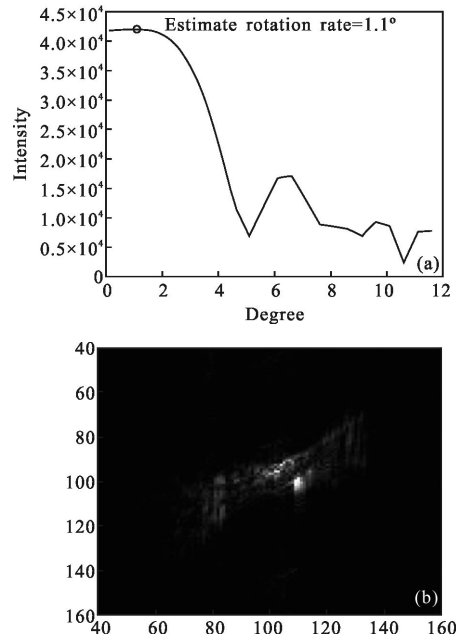range scale is given in Fig.8 (a) as a cross comparison. The pixel scale in these ISAR images is $0.5\,m×0.5\,m$.

Fig.7 Projection of the radar return on the frame at the prominent point versus target rotation rate. The maximum intensity appears at $\omega=1.1(°)/s$ and defocusing effect under FP imaging: ISAR image of B737 under FP method at a mismatched rotation rate $\omega=10(°)/s$
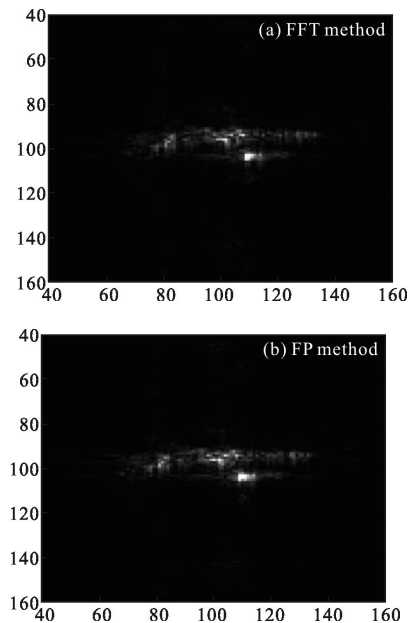

Fig.8 ISAR images at the estimated target rotation rate $\omega=1.1(°)/s$ on a Range-Cross Range plane. As ground truth ω_0 is unavailable, we judge the correctness of this estimated rotation rate by visual inspection and cross check with the result of an FFT method

Result discussion:

Along with the experiment, we also performed the target rotation vector magnitude estimation using the Minimum Entropy method as decribed in[19]. We observed that the result is consistent with that of the proposed prominent point method but with a larger variance induced by background noise.

We mention that if a global maximum value for a given ω range cannot be found, it is likely that the underlying target scatterer center is not a prominent point and should be removed from consideration.

Note that the usefulness of the proposed technique is limited as a prominent point is not always presented. In the case where a prominent point does not exist, one may consider other alternatives, such as the Minimum Entropy method mentioned above.

4　Conclusions

The target rotation rate in ISAR imaging is required for the determination of the cross-range scale of a reconstructed image. With an incorrect target rotation rate the reconstructed image can be distorted in different ways depending on the ISAR imaging technique used. Estimating this parameter from radar returns is important but a serious research challenge. In this paper, we show that Frame Processing based ISAR imaging method encapsulates an embedded target rotation model which provides a mechanism to estimate the rotation rate of a target under a maximum intensity criterion at a prominent scatterer. An analytical result based on relationship between the ground truth and reconstructed image derived using the FP method is presented in terms of a frame operator in an attempt to demonstrate the performance of ISAR imaging with respect to target rotation vector magnitude. A practical procedure for estimating the rotation vector magnitude of a non-cooperative target from radar returns is described and its effectiveness is justified from both simulated and real ISAR imaging scenarios.

References:

[1]　Yeh C M, Xu J, Peng Y N, et al. Rotational motion estimation for ISAR via triangle pose difference on two range-Doppler images [J]. *IET Radar, Sonar and Navigation*, 2010, 4(4): 528−536.

[2]　Martorella M. Novel approach for ISAR image cross-range scaling [J]. *IEEE Trans Aerospace and Electronic Systems*, 2008, 44(1): 281−294.

[3]　Yeh C, Yang J, Peng Y, et al. Rotation estimation for ISAR targets with a space time analysis technique [J]. *IEEE Geoscience and Remote Sensing Letters*, 2011, 8(5): 899−903.

[4]　She Z, Liu Y. Autofocus for ISAR imaging using higher order statistics [J]. *IEEE Geoscience and Remote Sensing Letters*, 2008, 5(2): 299−303.

[5]　Peng S B, Xu J, Peng Y N, et al. Inverse synthetic aperture radar rotation velocity estimation based on phase slope difference of two prominent scatterers [J]. *Radar, Sonar Navigation, IET*, 2011, 5(9): 1002−1009.

[6]　Mao Yeh C, Xu J, Peng Y N, et al. Cross-range scaling for isar via optical flow analysis [J]. *Aerospace and Electronic Systems Magazine, IEEE*, 2012, 27(2): 14−22.

[7]　Huang Y, Wang X, Li X, et al. Inverse synthetic aperture radar imaging using frame theory [J]. *IEEE Trans Signal Processing*, 2012, 60(10): 5191−5200.

[8]　Huang Y, Wang X, Li X, et al. Target rotation rate estimation via isar frame processing [J]. *Electronics Letters*, 2013, 49(6): 424−425.

[9]　Jakowatz C V J, Wahl D E, Eichel P H, et al. Spotlight-Mode Synthetic Aperture Radar: A Signal Processing Approach[M]. Boston: Kluwer Academic Publishers, 1996.

[10]　Desai M, Jenkins W. Convolution backprojection image reconstruction for spotlight mode synthetic aperture radar[J]. *Image Processing, IEEE Transactions on*, 1992, 1(4): 505−517.

[11]　Madisetti V. A fast spotlight-mode synthetic aperture radar imaging system[J]. *Communications, IEEE Transactions on*, 1994, 42(234): 873−876.

[12]　Huang Y, Wang X, Li X, et al. Tomographic radar imaging using frame theory [C]//15th International Conference on Information Fusion, 2012(S): 1421−1426, 9−12.

[13]　Gabor D. Theory of communication [J]. *Journal of the Institution of Electrical Engineers −Part III: Radio and Communication Engineering*, 1946, 93(26): 429−457.

[14] Duffin R J, Schaeffer A C. A class of nonharmonic fourier series [J]. *Transactions of the American Mathematical Society*, 1952, 72(2): 341−366.

[15] Lu G Y, Bao Z. Compensation of scatterer migration through resolution cell in inverse synthetic aperture radar imaging [J]. *IEE Proceedings-Radar Sonar and Navigation*, 2000, 147: 80−85.

[16] Xing M, Wu R, Bao Z. High resolution ISAR imaging of high speed moving targets [J]. *IEE Proceedings-Radar Sonar and Navigation*, 2005, 152: 58−67.

[17] Raj R, Farshchian M. Isar imaging in sea clutter via compressive sensing [C]//Waveform Diversity and Design Conference(WDD), 2010 International, 2010: 200−205.

[18] Tropp J, Gilbert A. Signal recovery from random measurements via orthogonal matching pursuit [J]. *Information Theory, IEEE Transactions on*, 2007, 53(12): 4655−4666.

[19] Li X, Liu G, Ni J. Autofocusing of ISAR images based on entropy minimization [J]. *IEEE Trans AES*, 1999, 35(4): 1240−1252.